Non-Linear Rheology and Return Flow in the Mantle

W. R. Jacoby[1] and G. Ranalli[2]

[1] Institut für Meterologie und Geophysik der Universität,
Feldbergstr. 47, D-6000 Frankfurt 1, Federal Republic of Germany
[2] Department of Geology, Carleton University Ottawa, Canada

Abstract. A simple model of mantle return flow in response to lithospheric plate motions is developed. Such a model is realistic if the buoyancy forces are concentrated in the plates. One-dimensionality is chosen as a simplification to study effects of mantle rheology in as much isolation as possible. Rheology is modelled as a combination of dislocation creep, diffusion creep and fluid phase transport; parameters are those appropriate for olivine. We have varied temperature, grain size, influence of partial melt, diffusivity and activation energy, grain deformation versus grain boundary sliding dominated creep, and surface plate velocity. A peculiar feature of non-linear rheology is the existence of low-stress high-viscosity regions, which, however, are of little dynamic importance because deformation there is very small. The main results are (1) that the model does not predict an excessive pressure gradient to be required by the return flow (which would be evident in a rise of the sea floor and strong increase in free air gravity anomalies toward the trenches); (2) that no excessive shear stresses at the plate bottom are predicted (which might result in observable heat flow effects and intra-plate seismicity and would require implausibly great driving forces at the plate ends); (3) that the model predicts the return flow to extend into the deeper mantle; this follows, however, from the simplifying assumption of olivine rheology below 400 km depth and would then argue for rather high temperatures, small grain sizes, possibly important fluid phase transport, and small activation volume. Recent work on the variation of activation volume with pressure and phase changes suggests a rather 'soft' lower mantle and thus supports the notion of 'deep' return flow. In interpreting the results one must, of course, keep in mind that the model is a purely mechanical one with a predetermined temperature profile (varied within plausible limits) and that the physics of the thermodynamic aspects of the flow problem is ignored.

Key words: Rheology of earth's mantle — Plate sections — Model of mantle flow.

Introduction

The present state of ignorance about plate dynamics requires model studies of mantle flow. One problem is that of the return flow: if a rigid surface plate moves in one direction the material below must flow back to conserve mass; in this model the plate moves against resistance from the return flow and drives it. The forces driving the plate, and the opposite model where the plate is carried passively or driven against some other resistance by the deep mantle flow, are not the subject of this paper.

In former studies (Schubert and Turcotte, 1972; Jacoby, 1978) depth-dependent Newtonian viscosity was assumed, but it is probably more realistic for the polycrystalline mantle to have non-Newtonian rheology (Stocker and Ashby, 1973). In order to isolate the effects of different rheologies it seems sensible, as done in the above studies, to model the problem in its simplest, i.e., one-dimensional and steady-state form; all quantities vary only with depth and the full circulation is ignored as though a 'cell' is infinite horizontally. The method of solution for non-linear rheology is an iterative one using the direct linear solution given by Jacoby (1978). Stresses and strain rates are found by successive adjustments and as one of the results one obtains the effective viscosity as their ratio. This viscosity is an integral part of the model and will not be appropriate to situations where additional strains are superimposed.

As will be discussed below, the non-linear creep of mantle material is strongly sensitive to temperature (among other parameters) so that shear heating will influence the flow. We have chosen to ignore this thermo-dynamic aspect of the problem in order to keep the model very simple; it is thus a purely mechanical one with predetermined temperature-depth profiles, varied within plausible limits. Schubert and Turcotte (1972), Froidevaux and Schubert (1975), Schubert et al. (1976), Froidevaux et al. (1977), Schubert et al. (1978), and Yuen et al. (1978) have treated the flow problem in a fuller way by including the shear heating and thus solving for temperature beside the flow velocity. As mentioned at the outset, the first of these papers assumed Newtonian viscosity; the later ones assumed non-linear dislocation creep but did not include diffusion creep and fluid phase transport because these would presumably be of little influence. In the simpler of their models the asthenosphere was assumed to be simply a layer of shear (not return) flow; the most complex model (Schubert et al., 1978; Yuen et al., 1978) additionally included partial return flow and vertical flow from below in variable proportions, buoyant forces, and heat advection. This is physically more complete than our model, but also more complex. Furthermore, there is still the unknown distribution of additional heat sources (other than dissipation) such that the complete thermodynamic solution of the flow problem remains open to ad hoc assumptions. We thus present our simple model as an instructive exercise in the study of the effects of various rheologies on the mantle return flow in a purely mechanical sense.

The method of solution and our assumptions, in particular those with respect to rheology, will be presented first. Then the results will be presented and discussed in terms of the geophysical constraints and consequences on gravity, sea floor topography, heat flow, plate kinematics, and stress in the lithosphere.

Method of Solution

In the one-dimensional steady-state return flow model (Jacoby, 1978) all quantities vary only with depth, z, and the horizontal (x) flow is driven entirely by the negative horizontal pressure (p) gradient balancing the resulting vertical gradient of the horizontal shear stress (τ)

$$\frac{\partial p}{\partial x} = \frac{\partial \tau}{\partial z}. \tag{1}$$

Effects of the rising and falling flow and of sphericity are neglected; gravity has no influence. The net transport through a vertical section is assumed to be zero. The surface velocity is imposed on the model and the bottom is held fixed at an arbitrary depth, for which we have usually chosen 2,000 km.

   If the viscosity is Newtonian,

$$\tau = \eta \frac{du}{dz} \tag{2}$$

and Eq. (1) can be solved if $\partial p/\partial x$ is an integrable function of z, e.g., $\partial p/\partial x = A$. For stepwise constant $\eta(z) = \eta_i$ for $z_i < z \leqq z_{i+1}$:

$$\tau = A z + \eta_i B_i \quad \text{and} \quad \eta_i B_i = B \tag{3}$$

B is the shear stress at the bottom of the surface plate. The flow velocity u becomes

$$u = \frac{A}{\eta_i} \frac{z^2}{2} + \frac{B}{\eta_i} z + C_i. \tag{4}$$

Assuming continuous velocity and shear stress we can compute C_i. The solution is linear in surface velocity u_l.

   If power law creep is assumed, $\tau^n = \beta \dfrac{du}{dz}$, where β is a PT-dependent parameter and n is a constant PT-independent exponent. Integration gives:

$$\tau = A z + \beta_i^{1/n} B_i = A z + B; \qquad u = \frac{(A z + B)^{n+1}}{A \beta_i (n+1)} + C_i. \tag{5}$$

For large n the velocity-depth profile approaches the cornered one of ideal plasticity. The problem is no longer linear in the surface velocity u_l.

   If diffusion *and* dislocation creep govern the effective viscosity, its stress dependence $\eta(\tau)$ is such that no simple analytical solution can be found. A convenient way to solve this non-linear problem is iteration of the linear solutions by progressively adjusting the effective viscosities on the basis of the stresses found in the previous steps. One starts with an arbitrary initial viscosity $\eta_0(z)$ and has found the correct viscosity when successive solutions no longer differ significantly. In this scheme the initial assumption $\eta_0(z)$ may be important for rapid convergence; we found it best to compute $\eta_0(z)$ with the assumed stress-dependence $\eta(\tau)$ and an anticipated stress distribution $\tau(z)$

Convergence was tested by the squared stress change integrated over the whole depth range and normalized with respect to the previous total stress integral:

$$\frac{\int_0^{z_m} \Delta\tau^2\,dz}{\int_0^{z_m} \tau^2\,dz} = \frac{\Delta A^2 z_m^2/3 + \Delta A\,\Delta B z_m + \Delta B^2}{A^2 z_m^2/3 + AB z_m + B^2} < \varepsilon. \tag{6}$$

The convergence was sometimes very slow if the solutions oscillated between two extremes: zero stress → high viscosity and, in turn, high stress → very low viscosity; once the solution approached the final one, convergence became rapid.

Rheology of the Upper Mantle

The effective viscosity used in the above procedure is the ratio of stress and strain rate and cannot be defined without discussion of the creep mechanisms. Experimental results on rock deformation (Carter, 1976), observation of flow textures in rocks of mantle origin (Nicolas, 1976), and theories of solid state creep (Weertman, 1970), show that dislocation creep, which leads to a power-law dependence of strain rate upon stress, is widespread, and may be predominant, in the upper mantle. Glacio-isostatic data can be fitted by the assumption of linear viscosity (Walcott, 1973) and equally well by a power-law model (Post and Griggs, 1973). If a liquid phase is present, diffusional flow through the liquid may become possible (Stocker and Ashby, 1973). Thus as a first approximation there are three creep mechanisms of possible relevance to polycrystals under upper mantle conditions: (i) diffusion creep, governed by the migration of vacancies through the grains (Nabarro-Herring creep) or along grain boundaries (Coble creep), which results in linear viscosity; (ii) dislocation creep, governed by dislocation climb and glide, which results in power-law creep; and (iii) fluid phase transport creep, when diffusion through the liquid (partial melt in the case of the asthenosphere) becomes predominant: it also results in linear viscosity. The results on strain rates and effective viscosities obtained by using the rheological parameters of olivine apply to the upper mantle only, and if extrapolated to the lower mantle must be treated with caution, since olivine goes through a series of phase changes in the mesosphere.

The equations govering the three types of creep can be written down as follows (Stocker and Ashby, 1973):

Dislocation creep: $\dot{\varepsilon} = \dfrac{(3^{1/2})^{n+1}}{2} A \dfrac{D\mu b}{kT} \left(\dfrac{\sigma}{\mu}\right)^n$ \hfill (7)

Diffusion creep: $\dot{\varepsilon} = 21 \dfrac{D_e \Omega\mu}{kTd^2} \left(\dfrac{\sigma}{\mu}\right)$ \hfill (8)

Fluid phase transport: $\dot{\varepsilon} = 21 \dfrac{D_f \Omega\mu}{kTd^2} \left(\dfrac{\sigma}{\mu}\right)$ \hfill (9)

where $\dot{\varepsilon}$ = shear strain rate; σ = shear stress;
D, D_e, D_f = diffusion coefficients;
A, n = Dorn's parameters; μ = rigidity; b = Burgers' vector; Ω = atomic volume;
k = Boltzmann's constant; T = absolute temperature; d = grain size.

The temperature and pressure dependence of the diffusion coefficient in dislocation creep is

$$D = D_0 \exp\left(-\frac{Q+pV}{RT}\right) \tag{10}$$

where Q = activation energy; V = activation volume; p = pressure; and R = gas constant. Activation energy and volume are those appropriate for lattice diffusion.

In diffusion creep, the diffusion coefficient is given by

$$D_e = D_V + \frac{\pi\delta}{d}D_B \tag{11}$$

where D_V and D_B are the diffusion coefficients for lattice and grain-boundary diffusion, respectively; δ = grain-boundary width; and d = grain size. The PT-dependence of D_V is assumed identical to (10); so is the form of the PT-dependence of D_B, but with activation energy about 1/3 less than the activation energy for lattice diffusion. The diffusion coefficient when fluid phase transport is present is given by

$$D_F = D_V + \frac{\pi\delta}{d} \cdot D_B + f \cdot C_L \cdot D_L \tag{12}$$

where f = volume fraction of the liquid phase; C_L = solubility of the diffusing species in the liquid; and $D_L = kT/8\eta_L\Omega^{1/3}$ is the diffusion coefficient in the liquid (η_L is the liquid viscosity).

In Eqs. (7), (8), and (9) the numerical constants are such that the invariant form of the creep laws is satisfied; $\dot{\varepsilon}$ and σ must be interpreted as shear strain rate and shear stress. If grain boundary sliding with diffusional accommodation is predominant over grain shape changes, the strain rate increases approximately sevenfold. This type of creep has been called 'superplastic' creep (Ashby and Verrall, 1973).

We approximate the upper mantle as a pure olivine layer (Fo_{90-95}). Table 1 lists the values of the rheological parameters adopted in this paper for dislocation and diffusion creep.

In the case of fluid phase transport, the estimation of rheological parameters is at least one order of magnitude less reliable than in solid phase creep. The liquid fraction, on the basis of seismological evidence (Anderson and Sammis, 1970), is taken to be of the order of 0.01. The diffusion coefficient in the liquid depends critically on the viscosity of the melt, and thus on the activation energy for viscous flow:

$$D_L = \frac{kT}{8\eta_L\Omega^{1/3}}, \quad \eta_L = A_\eta \exp\left(\frac{E_\eta}{RT}\right). \tag{13}$$

Table 1. Rheological parameters for olivine

	Parameter	Value	References
Dorn's parameter	A	0.7	[1]
Dorn's parameter	n	3.0	[1], [2], [4]
Burgers' vector	b	$6.98 \cdot 10^{-10}$ m	[1], [3]
pre-exponential diffusivity	D_0	10^{-1} m^2 s^{-1}	[3]
activation energy	Q	$5.4 \cdot 10^5$ J mol^{-1}	[1], [3]
activation volume	V	$1.1 \cdot 10^{-5}$ m^3 mol^{-1}	[1], [2]
atomic volume	Ω	$1.15 \cdot 10^{-29}$ m^3	[1], [3]
grain size	d	$10^{-4} - 10^{-2}$ m	[5]
grain boundary width	δ	$1.4 \cdot 10^{-9}$ m	[1]

[1] Stocker and Ashby, 1973; [2] Kirby and Raleigh, 1973; [3] Twiss, 1976; [4] Carter, 1976; [5] Nicolas, 1976

Experimental results (Murase and McBirney, 1973, Kushiro et al., 1976) suggest $E_\eta \approx 2 \cdot 10^5$ J·mol^{-1} and $A_\eta \approx 10^{-6}$ Pa·s. The resulting viscosities in the astheno-sphere, however, would be too low by about two orders of magnitude. It should be kept in mind that electroviscous effects may be important, by which the apparent viscosity of a polar liquid in a very thin channel is much larger than that of the bulk liquid. Furthermore grain boundary wetting may be incomplete and not all liquid channels may be interconnected. Therefore D_L [Eqs. (12) and (13)] has been calculated by taking $A_\eta = 10^{-4}$ Pa·s, but in view of the above effects, this is likely to give an upper limit for the influence of partial melting and the influence on the long term rheology of the asthenosphere may well be zero. Finally, the PT-dependence of the rigidity is taken as

$$\mu = \mu_0 \left[1 + \frac{1}{\mu_0} \frac{\partial \mu}{\partial T} (T - T_0) + \frac{1}{\mu_0} \frac{\partial \mu}{\partial p} (p - p_0) \right] \tag{14}$$

where (Stocker and Ashby, 1973):

$$\mu_0 = 7.9 \cdot 10^{10} \text{ Pa}; \qquad \frac{1}{\mu_0} \frac{\partial \mu}{\partial T} = -1.36 \cdot 10^{-4} \, K^{-1} \, (T \geqq 500 \, K);$$

$$\frac{1}{\mu_0} \frac{\partial \mu}{\partial p} = 2.25 \cdot 10^{-11} \text{ Pa}^{-1}.$$

This is probably accurate in the upper mantle, but there are discrepancies with the seismically determined rigidity in the lower mantle.

Summarizing Eqs. (7) to (14) and taking into account that in the present return flow problem $\dot{\varepsilon} = \frac{1}{2} \frac{du}{dz}$, we write

$$\eta = 1 / \{ C_1 \, \varphi_1(T, p) \cdot \tau^{n-1} + C_2 \, \varphi_2(T, p) + C_3 \, \varphi_3(T, p, f) \} \tag{15}$$

with

$$C_1 = 3^{\frac{n+1}{2}} A D_0 \, b / \mu_0^{n-1};$$

$$\varphi_1 = \exp\left(-\frac{Q+pV}{RT}\right)\bigg/\left\{ kT\left[1+\frac{1}{\mu_0}\frac{\partial \mu}{\partial T}(T-T_0)+\frac{1}{\mu_0}\frac{\partial \mu}{\partial p}(p-p_0)\right]^{n-1}\right\}$$

for dislocation creep;

$$C_2 = \alpha D_0 \, \Omega / d^2; \quad \varphi_2 = \exp\left(-\frac{Q+pV}{RT}\right)\left[1+\frac{\pi\delta}{d}\exp\left(\frac{Q/3}{RT}\right)\right]\bigg/ kT \qquad (16)$$

for diffusion creep; and

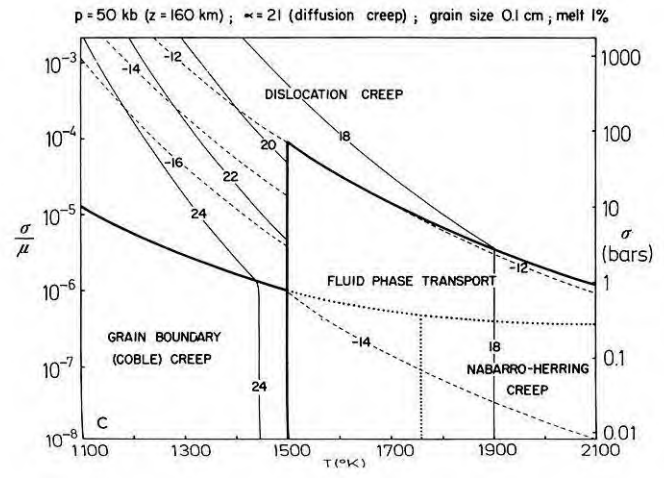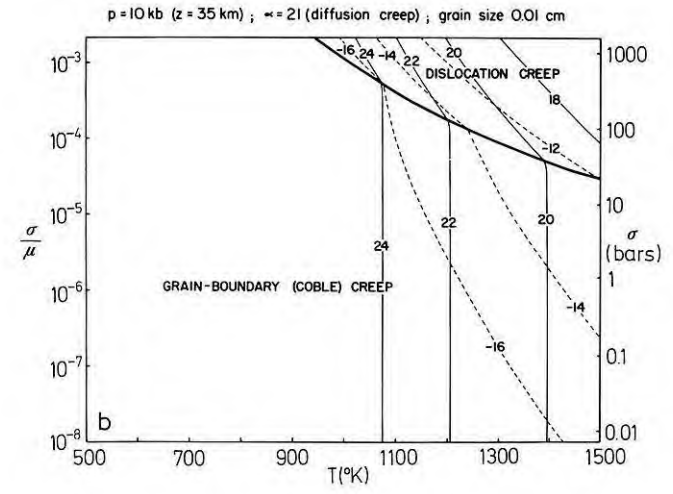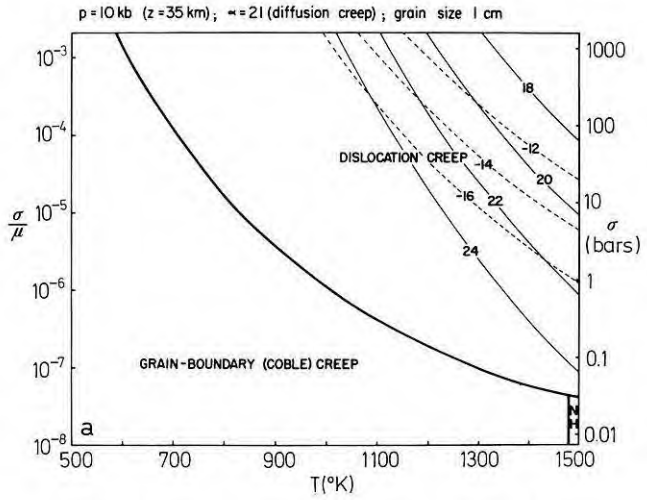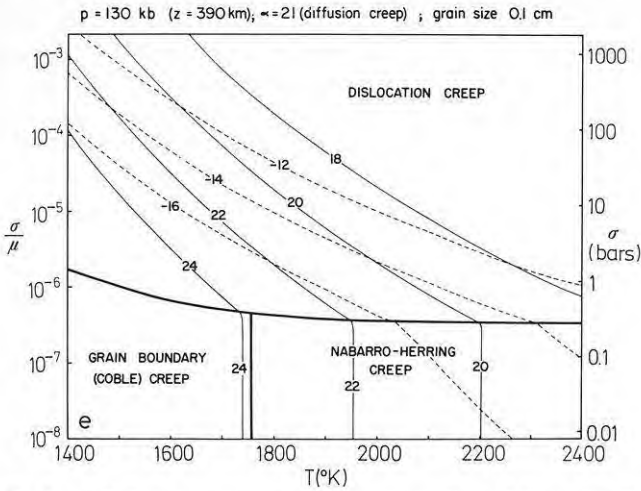$$C_3 = \frac{\alpha}{8} C_L \Omega^{2/3}/(A_\eta d^2); \quad \varphi_3 = f(z)\cdot\exp\left(-\frac{E_\eta}{RT}\right)$$

for fluid phase transport; when the equations are written in terms of u, the constant α is 42 if grain shape change dominates and 294 if grain boundary sliding dominates.

As in other studies (Stocker and Ashby, 1973; Kirby and Raleigh, 1973; Carter, 1976; Twiss, 1976; Durham and Goetze, 1977; Ashby and Verrall, 1977) the complex viscosity law (15) chosen is illustrated by 'deformation maps', showing the stress-temperature fields at various pressures (depths) in which one creep mechanism is predominant; a more detailed discussion is given elsewhere (Ranalli, 1978). The results are presented as a function of temperature; it is then possible to choose the temperature range appropriate for given depths and regions. (Alternatively, deformation maps may be computed as function of depth). Five examples are shown in Fig. 1a–e). The parameters assumed in each case are shown on the diagram. Curves of constant strain rates have been computed for $\dot{\varepsilon}$ from 10^{-16} to 10^{-11}s^{-1}, which should encompass most situations of geodynamic significance. Curves of constant effective viscosity have been computed for $\eta = 10^{16}, 10^{18}, \ldots, 10^{26}$ poise (10 poise $= 1 \text{ Pa}\cdot\text{s}$).

Figures 1a and b depict the situation within the lithosphere. Effective viscosities are larger than 10^{24} poise for realistic T and σ. It is interesting to note that at lower temperatures linear creep appears to be predominant: purely diffusive flow is sometimes termed 'presseure solution' by geologists, and direct observation of metamorphic rocks shows textures attributable to it (Elliott, 1973). Diffusion-type flow at lower temperatures is also greatly enhanced by the presence of water (Rutter, 1976). Figures 1c and d illustrate a possible situation in the asthenosphere. For grain sizes of 0.1 cm and about 1 % partial melt, the asthenosphere behaves linearly at stresses of a few bars or less; dislocation creep is still predominant at higher stresses. If the grain size is larger and the melt fraction smaller, dislocation creep is predominant at all stresses above a few tenths of a bar. Strain rates and effective viscosities are as inferred from tectonic and glacio-isostatic processes. Figure 1e shows the conditions prevailing below the asthenosphere. The main result is that, below the asthenosphere, dislocation creep is predominant at all stresses above a few tenths of a bar.

p = 10 kb (z = 35 km) ; ∝ = 21 (diffusion creep) ; grain size 1 cm

a — DISLOCATION CREEP; GRAIN-BOUNDARY (COBLE) CREEP

p = 10 kb (z = 35 km) ; ∝ = 21 (diffusion creep) ; grain size 0.01 cm

b — DISLOCATION CREEP; GRAIN-BOUNDARY (COBLE) CREEP

p = 50 kb (z = 160 km) ; ∝ = 21 (diffusion creep) ; grain size 0.1 cm ; melt 1%

c — DISLOCATION CREEP; GRAIN BOUNDARY (COBLE) CREEP; FLUID PHASE TRANSPORT; NABARRO-HERRING CREEP

p = 50 kb (z = 160 km) ; ∝ = 21 (diffusion creep) ; grain size 1 cm ; melt 0.1 %

d — DISLOCATION CREEP; GRAIN BOUNDARY (COBLE) CREEP; FLUID PHASE TRANSPORT; NABARRO-HERRING CREEP

p = 130 kb   (z = 390 km); ≼ = 21 (diffusion creep) ; grain size 0.1 cm

Fig. 1a–e. Deformation maps: *thick continuous lines:* deformation field boundaries; *thin continuous lines:* effective viscosities (as powers of ten); *dashed lines:* strain rates (also as powers of ten). **a** for $z = 35$ km, $d = 1$ cm; **b** $z = 35$ km, $d = 0.01$ cm; **c** $z = 160$ km, $d = 0.1$ cm, and 1 % partial melting (*the dotted lines* represent the extensions of dislocation diffusion fields if fluid phase transport were absent); **d** $z = 160$ km, $d = 1$ cm, partial melting 0.1 %; **e** $z = 390$ km, $d = 0.1$ cm
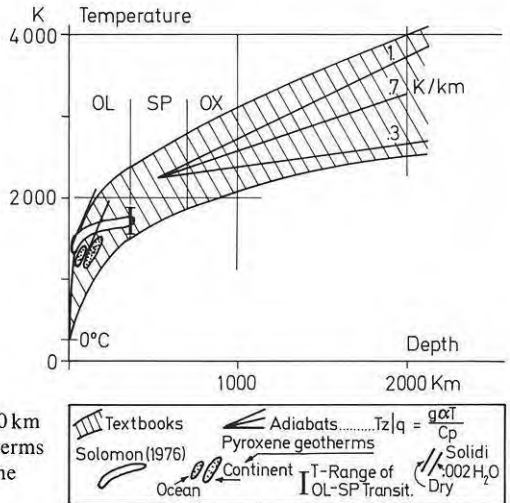
Fig. 2. Temperature range in the mantle to 2,000 km depth; for references see Solomon (1976). Geotherms assumed in model computations are shown in the following figures

In summary, the effective viscosity law we assume has the following main features. In the absence of partial melting, dislocation creep is predominant at high stresses and diffusion creep at small stresses. Superplasticity increases the temperature-dependent transition stress by a factor less than three. An increase in grain size by one order of magnitude decreases the transition stress by approximately the same amount. Within the diffusion creep field an increase in

grain size favours Nabarro-Herring over Coble creep; the latter is predominant at lower temperatures. Pressure has no effect over field boundaries, if the pressure-dependence of the various diffusion coefficients is the same; we take this as a simplifying assumption. If a liquid phase with complete grain-boundary wetting is present, fluid phase transport is always predominant over diffusion creep within the linear field; if, however, electroviscous phenomena were more important in the asthenosphere than assumed here, it may have no relevance at all for mantle rheology (naturally excluding situations in which the melt fraction is much larger than 0.01). Fluid phase transport raises the transition stress between non-linear and linear creep, but at high stresses dislocation creep is always predominant.

As Fig. 1 demonstrates temperature is one of the most critical parameters; the return flow profiles will depend very strongly on the geotherms chosen. Since temperature in the earth is poorly known we have assumed a whole range of geotherms, shown in Figure 2. The upper mantle temperatures are constrained by geophysical and geological observations (Solomon, 1976), but the range of possible lower mantle temperatures is wide. It is often assumed that, because of steady-state convection, the temperature in the deeper mantle is slightly super-adiabatic; the adiabatic gradient is given by $g \alpha T/c_p \approx 0.3 - 0.6$ K/km (gravity $g \approx 10$ m/s^2; thermal volume expansion $\alpha \approx 1 - 2 \cdot 10^{-5}$ K^{-1}; heat capacity $c_p \approx 800$ J/kg $\cdot$ K; absolute temperature $T \approx 2000$ K); for the Rayleigh number to be at least critical (Ra$_c \approx 2,000$), only a very small quantity has to be added: $(\text{Ra}_c \cdot \kappa v)/(\alpha g d^4) \approx 10^{-2}$ K/km (thermal diffusivity $\kappa \approx 1.5 \cdot 10^{-4}$ m^2/s, kinematic viscosity $v \approx 10^{17}$ m^2/s, depth of convecting layer $d \approx 2,000$ km). The assumption of internal convection, superimposed on the return flow, is however, self-defeating for our model with non-linear rheology, since the additional strains will alter the effective viscosity. The one-dimensional return flow model clearly cannot simulate realistic mantle flow; what we want to do is to investigate how a mantle of 'realistic' rheology reacts to such a simple model. The geotherms assumed in each of the models presented below are given on the diagrams.

Non-Linear Return Flow Models: Results

We shall first discuss the influence of temperature on the return flow by assuming a set of geotherms within the range of Fig. 2. Other parameters also varied within plausible limits will be discussed subsequently; these involve the pre-exponential diffusivity D_0 and the activation energy Q; the constant α for grain deformation and grain boundary sliding dominated creep, and the influence of partial melt. All models were computed for three grain sizes $d = 1, 3, 10$ mm and three surface plate velocities $u_l = 1, 3, 10$ cm/a. The power of the dislocation creep term has always been assumed $n = 3$. The results are presented in the form of depth profiles (Fig. 3–6) of horizontal flow velocity $u(z)$ and effective viscosity $\eta(z)$ together with the assumed geotherms $T(z)$. Other important parameters assumed fixed are shown on the lower lefthand side of the diagrams. Also given, at the bottom, are the computed pressure gradient A or its equivalent gravity

gradient in mgal/10,000 km and the shear stress B at the bottom of the model surface plate.

Figure 3 compares five geotherms with lower-mantle gradients of 0.5, 0.6, 0.75, 0.9, and 1 K/km; surface velocity is 3 cm/a, grain sizes are 1, 3, and 10 mm. As the temperature gradient is raised, the effective viscosities and stresses generally become smaller and the return flow occurs at greater depth (260 to 540 km) and broadens (with decreasing amplitude). In no model is the return flow concentrated in the asthenosphere of minimum viscosity ($2 \cdot 10^{19}$ Pa·s between 150 and 250 km depth in all models). In all model situations the viscosity minimum is caused by the dominance of temperature over pressure and dislocation creep is more important than diffusion creep. Below the asthenosphere lies a region of maximum return flow and small stresses; diffusion creep dominates below a few tenths of a bar. For small grain sizes ($\lesssim 1$ mm) viscosity remains nearly constant at $< 10^{21}$ Pa·s over several hundred kilometers in all models (over 500 km for $u_l = 1$ cm/a and $dT/dz = 1$ K/km). For grain sizes $d > 1$ mm (see e.g., $d = 10$ mm in Fig. 3) viscosity rises to a maximum in the shear-free fiber but the width of the zone of dominant superplastic diffusion creep (i.e., maximum diffusion creep in the absence of melt) narrows as grain size and surface velocity increase; and the maximum viscosity grows as d^2. Although effective viscosity is so different, the return flow profiles $u(z)$ are hardly affected by grain size, except for slight squaring for large d. At greater depths dislocation creep takes over again and in all models with large (small) grain size the effective viscosity goes to a second minimum (remains rather constant) near 10^{21} Pa·s before pressure makes it rise. Deeper down, this rise is nearly linear with depth for log viscosity; its magnitude is strongly dependent on the temperature gradient leading to many orders of magnitude viscosity difference at 2,000 km ($\sim 10^{29}$ Pa·s for 0.5 K/km versus $\sim 10^{22}$ Pa·s for 1 K/km). Accordingly, the depth extent of the return flow varies from model to model by a factor of 2. This result is hardly affected by difference in stress level for different surface velocities. The peculiar feature of two low viscosity channels may be typical of non-linear flow where temperature and stress are important at different depths.

If the viscosity-temperature relationship found for the deeper mantle appears unrealistic and lower viscosities are to be obtained with the low temperature gradients (e.g., 0.5 K/km), it should be noted that olivine parameters are not appropriate for the deep mantle. The simplest escape from the dilemma would be an activation volume decreasing with depth (e.g., about 30% at 2,000 km). This is indeed likely (O'Connell, 1977; Sammis et al., 1978).

Shear stress B (Fig. 3, bottom) at the plate bottom varies approximately as the inverse of the lower-mantle temperature gradient. Its depth variation is linear (for 0.5 K/km from $+7$ to -50 bar at 2,000 km; for 1 K/km from $+3$ to -8 bar; surface velocity $u_l = 3$ cm/a and all grain sizes considered). Thus even in the most unfavorable case of very high viscosities in the lower mantle the stresses are not excessive. The horizontal pressure gradient A inherent in the return flow model can be roughly transformed into a gravity gradient in the direction of motion across a moving plate (Schubert and Turcotte, 1972; Jacoby, 1978). The computed results are given on Fig. 3, bottom ($A \rightarrow \Delta g$) in

mgal/10,000 km and should be compared to the crude figure of 30 mgal/10,000 km across the Pacific plate, found by Woollard (1975). By this criterion nearly all models fail; only the model with a temperature gradient of 1 K/km gives acceptable gravity gradients of 15, 23, and 34 mgal/10,000 km for surface velocities of 1, 3, and 10 cm/a, respectively. These results are insensitive to grain size. The deep-mantle viscosities of the other models are too large for the return flow model to work. As discussed above, these models would, however, also work if activation volume decreases with depth.
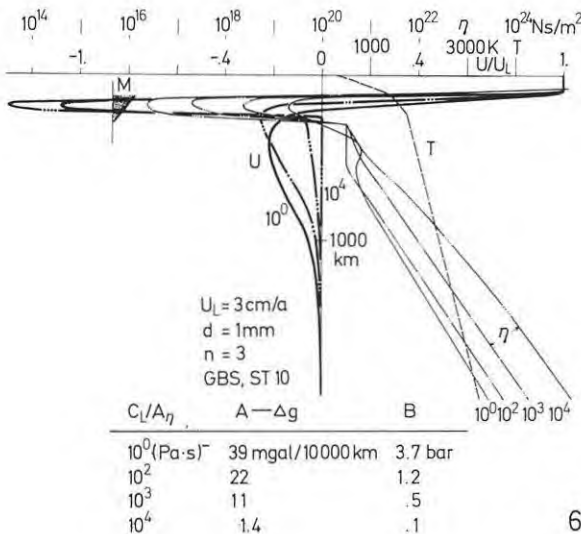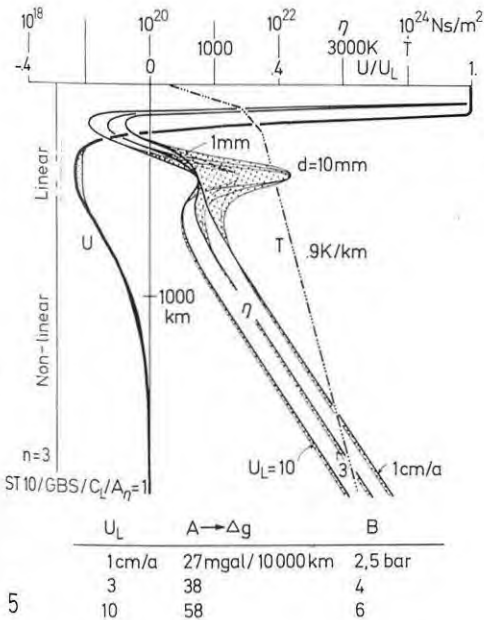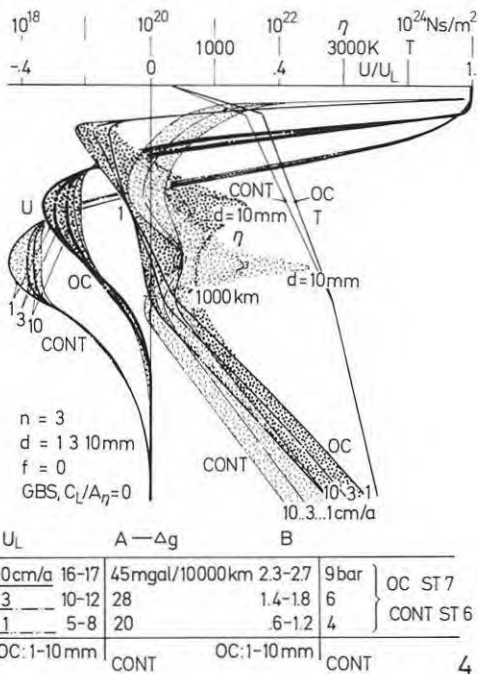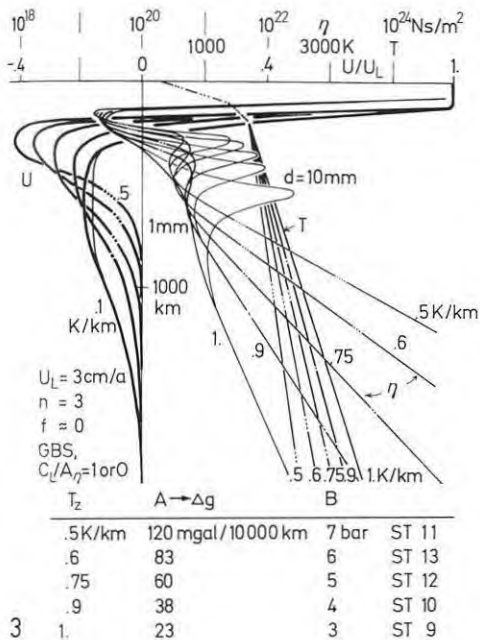
It would be interesting to compare 'oceanic' and 'continental' geotherms. An illustration of the effects is given in Fig. 4. We have assumed two geotherms differing by 250 K at 150 km depth; the difference decreases linearly to zero at 50 and 1,000 km. Such a choice may be more in line with Jordan's (1975) arguments for considerable temperature differences to great depths, than with Solomon (1976) and Duschenes and Solomon (1977). If the difference between oceanic and continental geotherms disappears at shallower depths than in our models the effects will be smaller than discussed here. The two models differ clearly in the depth of the return flow and in the effective viscosities at depths shallower than 1,000 km. At 'asthenospheric' levels the viscosity difference is more than an order of magnitude. For large grain sizes the effective viscosities near the maximum return flow are always relatively large. Below 1,000 km depth the 'oceanic' viscosities are slightly greater than the 'continental' ones because of the smaller stresses if the same plate velocity is assumed. But a 10 cm/a oceanic plate leads to the same effective viscosity as a 1 cm/a continental one. While the 'oceanic' stresses near the surface are only a few bars, and depend slightly on grain size, 'continental' stresses are between 4 and 10b for 1 to 10 cm/a surface velocity independent from grain size. The gravity gradients computed are smaller than 30 mgal/10,000 km for all 'oceanic' models but exceed this value for the 10 cm/a 'continental' one.

Fig. 3. Effect of temperature (T) gradient in lower mantle on return flow (u) and effective viscosity (η); thick curves for grain size $d = 1$ mm, thin lines for $d = 10$ mm. Other parameters as listed; *GBS:* indicates grain boundary sliding diffusion creep; *ST10 etc.:* indicate that the small pre-exponential diffusivity D_0 of Table 1 has been used together with geotherm no. *T10*, etc. For discussion, particularly of results *A, B (bottom)*, see text

Fig. 4. Effect of continental versus oceanic geotherm (T) on return flow (u) and effective viscosity (η), Bands marked by dots *(oceanic)* and by short lines *(continental)* indicate whole range of solutions for varying grain size $d = 1$ to 10 mm and lithospheric velocity $u_l = 1$ to 10 cm/a. Other parameters as listed. *GBS, ST6, ST7:* see caption of Fig. 3

Fig. 5. Effect of lithospheric velocity u_l (1, 3, 10 cm/a) on return flow (u) and effective viscosity (η) for given geotherm (T), grain size $d = 1$ to 10 mm *(dotted band of solutions)*, negligible melt influence and power $n = 3$ of power law; *ST10, GBS:* see caption of Fig. 3

Fig. 6. Effect of melt (M) on return flow (u) and viscosity (η); geotherm (T), lithospheric velocity u_l, grain size d, and power assumed as shown. For discussion of parameter as well as of results see text. *GBS, ST10:* see caption of Fig. 3

Figure 3:

10^{18} 10^{20} 10^{22} η 10^{24}Ns/m^2
1000 3000K T
-.4 0 .4 U/U$_L$ 1.

U .5 d=10mm
1mm T
1000 km
.1 K/km 5K/km
1. .9 .75 .6
U_L = 3cm/a
n = 3
f = 0
GBS, C_L/A_η=1 or O
.5 .6 .75 .9 1.K/km

T_z	A→Δg	B	
.5K/km	120 mgal/10000 km	7 bar	ST 11
.6	83	6	ST 13
.75	60	5	ST 12
.9	38	4	ST 10
1.	23	3	ST 9

3

Figure 4:

10^{18} 10^{20} 10^{22} η 10^{24}Ns/m^2
1000 3000K T
-.4 0 .4 U/U$_L$ 1.

U CONT OC d=10mm
1 T η
OC d=10mm
1000 km
1 3 10
CONT
n = 3
d = 1 3 10mm
f = 0
GBS, C_L/A_η=0
OC
CONT 10·3·1
10..3..1cm/a

U_L	A—Δg		B		
10cm/a	16-17	45mgal/10000km	2.3-2.7	9bar	OC ST 7
3	10-12	28	1.4-1.8	6	CONT ST 6
1	5-8	20	.6-1.2	4	
OC: 1-10 mm	CONT		OC:1-10mm	CONT	

4

Figure 5:

10^{18} 10^{20} 10^{22} η 10^{24}Ns/m^2
1000 3000K T
-.4 0 .4 U/U$_L$ 1.

Linear
1mm d=10mm
U T .9K/km
1000 km η
Non-linear
n=3
ST10/GBS/C_L/A_η=1 U_L=10 3 1cm/a

U_L	A→Δg	B
1cm/a	27mgal/10000 km	2,5 bar
3	38	4
10	58	6

5

Figure 6:

10^{14} 10^{16} 10^{18} 10^{20} 10^{22} η 10^{24}Ns/m^2
1000 3000K T
-1. -.4 0 .4 U/U$_L$ 1.
M T
U 10^4
10^0
10^0 1000 km
U_L=3cm/a
d = 1mm
n = 3
GBS, ST 10 η
$10^0 10^2 10^3 10^4$

C_L/A_η	A—Δg	B
10^0(Pa·s)$^-$	39 mgal/10000 km	3.7 bar
10^2	22	1.2
10^3	11	.5
10^4	1.4	.1

6

The influence of surface velocity u_l is illustrated by Fig. 5. Where dislocation creep is dominant the logarithmic viscosity-depth profiles are simply shifted, i.e., the viscosities are decreased by a constant factor, if the surface velocity is increased (1/6 or 1/7 for 10-fold increase of u_l) because the stresses are increased (by a factor of 2 or 3). Where diffusion creep dominates (for small grain sizes near the return flow maximum) the effective viscosities become nearly independent from u_l (but grow with grainsize d squared). The influence of plate velocity on the shape of the return flow profiles is hardly noticeable, but the pressure (A) and gravity (Δg) gradients increase [by a factor of (only) 2 for u_l changing from 1 to 10 cm/a].

The effect of grain size has already been discussed in connection with Figs. 3–5. Viscosity is affected only where the stress level is a fraction of a bar. The other parameters as the flow profile, shear stress, and pressure gradient are only slightly affected in our models. Grain sizes would have to be one or two orders of magnitude smaller than 1 mm for diffusion creep to become dominant everywhere and to affect the whole model results.

So far diffusional superplasticity (grain boundary sliding accommodated diffusion creep) was assumed. Had we assumed grain deformation dominated Nabarro-Herring and Coble creep, the influence of diffusion creep on the total deformation would be even smaller than found. The results would hardly change. In a test computation none of the quantities computed changed by more than 10%, except in the case with the smallest stresses ($u_l = 1$ cm/a, $d = 1$ mm and 'hot oceanic' mantle) where superplasticity leads to nearly 50% reduction of stresses and pressure gradient over Nabarro-Herring and Coble creep.

An attempt to estimate the influence of partial melting in the asthenosphere is presented in Fig. 6. It is widely believed that incipient melting occurs there if a fraction of one precent of H_2O is present, because temperature probably exceeds the wet solidus of peridotite (e.g., Solomon, 1976). For some of the geotherms discussed above, we have computed models with a melt fraction $f(z)$ of 1% at 100 km depth decreasing to zero at 250 km; we have assumed the poorly known ratio C_L/A_η (determining the importance of fluid phase transport in Eqs. (12), (13), and (16) to take on the values 0 (no importance), 1, 10, 10^2, 10^3 (preferred value, see above), 10^4, and 10^5 $(Pa \cdot s)^{-1}$ (value expected from bulk viscosity of basic melts).

The computed flow profile $u(z)$ and viscosity $\eta(z)$ are presented in Fig. 6 for the geotherm, surface velocity, and grain size as indicated. As expected, the presence of melt in the asthenosphere by lowering its effective viscosity facilitates the return flow by requiring a lower pressure gradient. If, however, $C_L/A_\eta \leq 1$ $(Pa \cdot s)^{-1}$, 1% of melt has no noticable effect. From $C_L/A_\eta = 1$ to 100, 1,000, 10,000 ... $(Pa \cdot s)^{-1}$ the effective viscosity in the layer with about 1% melt is decreased by 1, 2, 3, ... orders of magnitude, the stresses are lowered, and the return flow maximum is shifted upward into the layer with melt. It becomes the channel of dominant return flow for C_L/A_η between 100 and 1,000 $(Pa \cdot s)^{-1}$ and carries the total return flow for $C_L/A_\eta \geq 10,000$ $(Pa \cdot s)^{-1}$. Because of the stress reduction the effective viscosity rises in the lower mantle until linear diffusion creep dominates at all depths. The gravity gradients drop from
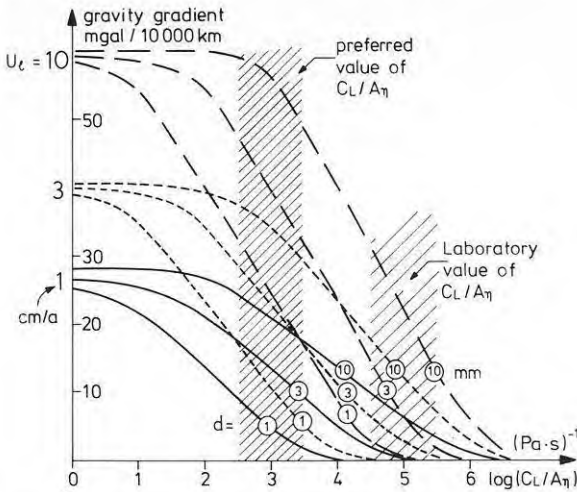
Fig. 7. Influence of 1% melt on pressure gradient shown by equivalent gravity gradient of return flow as a function of fluid phase transport parameter C_L/A_η (*Kabscissa*), surface plate velocity u_l (*parameter shown on lefthand side*), and grain size (*parameter shown by circled numbers at each curve*). The upper turning region of each curve marks the beginning of melt influence; the lower turning region marks that of total dominance of flow system by melt in asthenosphere

38 mgal/10,000 km (no melt) to essentially zero. The values of C_L/A_η where the effects of fluid phase transport first become noticeable and where the return flow becomes confined to the channel depend on grain size, and, to a minor degree, on plate velocity and temperature. This is illustrated in Fig. 7 by the gravity gradients $\Delta g/10,000$ km for all models computed with the same geotherm as that of Fig. 6, but varying u_l and d. The individual Δg-curves are asymptotic to the value appropriate to no melt for small C_L/A_η, then turn down to turn again approaching zero asymptotically for large C_L/A_η. The two turning regions indicate the beginning of melt effects and the beginning of their total dominance. Beyond, viscosity continues to decrease in the channel but the return flow profile is no longer affected. The 'turning regions' of C_L/A_η are proportional to d^2 for constant u_l and they increase as u_l for large d but are hardly affected by u_l for small d. It turns out that the preferred C_L/A_η value of $10^3 (\text{Pa} \cdot \text{s})^{-1}$ lies in the region of important but not total melt influence. It depends on too many factors for an evaluation to be possible at present, but since our model probably gives an upper limit, we feel safe to suggest that a dominant influence of 1% melt on the return flow is unlikely but that it could be of some importance for small grain sizes and plate velocities.

Finally we want to discuss whether or not the uncertainty of diffusivity D_0 and activation energy Q is critical to our model. We computed a number of models with both the values given in Table 1 and the ones given by Stocker and

Ashby (1973): $D_0 = 120 \, \text{m}^2/\text{s}$ and $Q = 6.4 \cdot 10^5 \, J \, \text{mol}^{-1}$; both pairs of values reasonably fit the laboratory data. In the majority of computations the Stocker and Ashby values lead to smaller stresses and pressure gradients; the difference was, however, not very significant; only for high temperature, small plate velocity and small grain size, i.e., for small stresses was the relative change by a factor of 1/5 or so.

Discussion

Although we cannot simulate realistic mantle flow with the one-dimensional model, we have been able to study the influence of rheological parameters of olivine, grain size, melt fraction, temperature, stress, and plate velocity. The results are more directly applicable to large plates than to small ones; but if the model works with an infinite plate it is likely to work with a finite one too (see Davies, 1977 a and b).

In an earlier study of the return flow model (Jacoby, 1978) it had been shown that the model is not in conflict with geophysical observations as gravity, sea floor topography, heat flow, and lithospheric stress, if plausible mantle viscosities are assumed which are based on glacio-isostatic rebound data (e.g. Walcott, 1973; Post and Griggs, 1973; Brennen, 1974; Peltier, 1974; Cathles, 1975; Peltier and Andrews, 1976; Peltier et al., 1978). Another result had been that the return flow may well extend to great depths in the mantle (Jacoby, 1978; see also Davies, 1977 a and b).

The main conclusions of the present study largely agree with those of the earler one. If non-linear olivine rheology is assumed the return flow model works equally and the return flow is likely to extend to depths well below the asthenosphere. In other words, olivine rheology in connection with plausible assumptions on temperature and grain size leads to similar effective viscosities in the return flow model as those found from glacial rebound (similar strain rates). This is opposite to what was found for exclusive diffusion creep rheology by Schubert and Turcotte (1972) who thence suggested that dislocation creep ough to be considered. The suggestion is borne out by the present models in which dislocation creep was generally dominant over diffusion creep, and also by the models of Froidevaux and Schubert (1975), Schubert et al. (1976), Froidevaux et al. (1977), Schubert et al. (1978), and Yuen et al. (1978), who assumed only dislocation creep of olivine. An interesting result of the two last papers mentioned was that under many circumstances the pressure gradient of the return flow is rather constant with depth; we mention in passing that this is an a posteriori justification for our arbitrary choice of this asssumption.

Results obtained for the deep mantle must be regarded with special caution since the rheological parameters of olivine assumed are not likely to be correct there. If they are correct, our model results favour a high temperature gradient (order 1 K/km), very small grain size (<0.1 mm), and/or important fluid phase transport in the asthenosphere. Alternatively a decrease of the activation volume (describing the pressure influence on the creep) with depth is suggested; this is

supported by the work of O'Connell (1977) and Sammis et al. (1977). Some of their estimates give such a strong decrease of the activation volume that temperature gradients as low as 0.3 K/km would still lead to acceptably low viscosities (and plausible return flow solutions). If these estimates are correct, our model results lead us to speculate that the return flow may extend deep into the lower mantle with the asthenosphere being essentially a "decoupling" layer of shear flow, in line with Davies' (1977a) conclusions.

Some of the particular features of non-Newtonian rheology deserve a little more discussion. One obvious effect is that stresses and pressure gradients are not linear with plate velocity. If grain size is greater than 1 mm we can expect these quantities to grow by a factor of only 2 to 3 when plate velocity increases from 1 to 10 cm/a. Gravity gradients and lithospheric stress should thus not strongly depend on plate velocity. Shear heating, not included in our model, would weaken this dependency further. The model implies stresses of the order of a few hundred bars in the lithosphere, because the surface plate must be driven from its ends (ridge, trench) to balance and maintain the shear stress B at its bottom; an oceanic plate 100 km thick and 10,000 km long would suffer a maximum (compressive or tensile) stress of $100 \cdot B$ and B was usually of the order of a few bars. The shear stress under continental plates is greater than under oceanic ones, if our assumptions concerning the geotherms are not grossly wrong. Considering the uncertainties, we estimate the difference to be roughly by a factor three. The maximum (compressive or tensile) stress for a continental plate 3,000 km long would thus be of the same order of magnitude as that in an oceanic plate 10,000 km long.

Regions of low-stress high viscosity are characteristic of non-linear viscosity. The important point is that this is dynamically irrelevant. In the low-stress regions there is so little deformation that further reduction because of non-linearity makes little difference in the flow distribution. In large regions with intermediate stress the effective viscosity does not vary very much; the assumption of Newtonion viscosity will thus not lead to gross errors. In small regions, however, of high stress, e.g., in descending slabs, non-Newtonian rheology may be critical to the solutions (Schmeling and Jacoby, in preparation). Superposition of additional strains (not considered in our model) will generally tend to 'soften' the mantle.

The major unknowns in modelling mantle dynamics are temperature, grain size, activation volume, and the physics of fluid phase transport. The return flow is facilitated by high temperature, small grain size, small activation volume, and fluid phase transport, or a combination of these. Jumps in activation energy and activation volume may be important too; they should be taken into account in future models.

References

Anderson, D.L., Sammis, C.: Partial melting in the upper mantle. Phys. Earth Planet. Inter. **3**, 41–50, 1970

Ashby, M.F., Verrall, R.A.: Diffusion-accommodated flow and superplasticity. Acta Metall. **21**, 149–163, 1973

Ashby, M.F., Verrall, R.A.: Micromechanisms of deformation and fracture, and their relevance to the rheology of the upper mantle. Philos. Trans. R. Soc. London, Ser. A: **288**, 59–95, 1977

Brennen, C.: Isostatic recovery and the strain rate dependent viscosity of the earth's mantle. J. Geophys. Res. **79**, 3993–4001, 1974

Carter, N.L.: Steady-state flow of rocks. Rev. Geophys. Space Phys. **14**, 301–360, 1976

Cathles, III, L.M.: The viscosity of the earth's mantle. Princton, N.J.: Princton Univ. Press, 386 pp., 1975

Davies, G.F.: Whole mantle convection and plate tectonics. Geophys. J. R. Astron. Soc. **49**, 459–486, 1977a

Davies, G.F.: Viscous mantle flow under moving lithospheric plates and under subduction zones. Geophys. J. R. Astron. Soc., **49**, 557–563, 1977b

Durham, W.B., Goetze, C.: Plastic flow of oriented single crystals of olivine. J. Geophys. Res. **82**, 5737–5753, 1977

Duschenes, J.D., Solomon, S.C.: Shear wave travel time residuals from oceanic earthquakes and the evolution of the oceanic lithosphere. J. Geophys. Res. **82**, 1985–2000, 1977

Elliott, D.: Diffusion flow laws in metamorphic rocks. Bull. Geol. Soc. Am. **84**, 2645–2664, 1973

Froidevaux, C., Schubert, G.: Plate motion and structure of the continental asthenosphere: a realistic model of the upper mantle. J. Geophys. Res. **80**, 2553–2564, 1975

Froidevaux, C., Schubert, G., Yuen, D.A.: Thermal and mechanical structure of the upper mantle: a comparison between continental and oceanic models. Tectonophysics **37**, 233–246, 1977

Goetze, C.: A brief summary of our present-day understanding of the effect of volatiles and partial melt of the upper mantle. In: High Pressure Research Applications in Geophysics, M. Manghnani and S. Akimoto (eds.), pp. 3–23. New York: Academic Press 1977

Jacoby, W.R.: One-dimensional modelling of mantle flow. Pure Appl. Geophys. **116**, 1231–1249, 1978

Jordan, T.H.: The continental tectosphere. Rev. Geophys. Space Phys. **13**, 1–12, 1975

Kirby, S.H., Raleigh, C.B.: Mechanisms of high-temperature, solid-state flow in minerals and ceramics and their bearing on the creep behaviour of the mantle. Tectonophysics **19**, 165–194, 1973

Kushiro, I., Yoder, H.S. Jr., Mysen, B.O.: Viscosities of basalt and andesite melts at high pressures. J. Geophys. Res. **81**, 6351–6356, 1976

Murase, T., McBirney, A.R.: Properties of some common igneous rocks and their melts at high temperatures. Bull. Geol. Soc. Am. **84**, 3563–3592, 1973

Nicolas, A.: Flow in upper mantle rocks: some geophysical and geodynamical consequences. Tectonophysics **32**, 93–106, 1976

O'Connell, R.J.: On the scale of mantle convection. Tectonophysics **38**, 119–136, 1977

Peltier, W.R.: The impulse response of a Maxwell earth. Rev. Geophys. Space Phys. **12**, 649–669, 1974

Peltier, W.R., Andrews, J.T.: Glacial-isostatic adjustment – I. The forward problem. Geophys. J. Roy. Astron. Soc. **46**, 605–646, 1976

Peltier, W.R., Farrell, W.E., Clark, J.A.: Glacial isostasy and relative sea level: a global finite element model. Tectonophysics **50**, 81–110, 1978

Post, R.L., Griggs, D.T.: The earth's mantle: evidence for non-Newtonian flow. Science **181**, 1242–1244, 1973

Ranalli, G.: Regional models of the steady-state rheology of the upper mantle. In: Earth rheology, isostasy and eustasy, N.A. Mörner (ed.) New York: Wiley 1978 (in press)

Rutter, E.H.: The kinetics of rock deformation by pressure solution. Philos. Trans. R. Soc. London, Ser. A.: **283**, 203–219, 1976

Sammis, C.G., Smith, J.C., Schubert, G., Yuen, D.A.: Viscosity-depth profile of the earth's mantle: effects of polymorphic phase transitions. J. Geophys. Res. **82**, 3747–3761, 1977

Schubert, G., Turcotte, D.L.: One-dimensional model of shallow convection. J. Geophys. Res. **77**, 945–951, 1972

Schubert, G., Froidevaux, C., Yuen, D.A.: Oceanic lithosphere and asthenosphere: thermal and mechanical structure. J. Geophys. Res. **81**, 3525–3540, 1976

Schubert, G., Yuen, D.A., Froidevaux, C., Fleitout, L., Souriau, M.: Mantle circulation with partial shallow return flow: effects on stresses in oceanic plates and topography of the sea floor. J. Geophys. Res. **83**, 745–758, 1978

Solomon, S.C.: Geophysical constraints on radial and lateral temperature variations in the upper mantle. Am. Mineral. **61**, 788–803, 1976

Stocker, R.L., Ashby, M.F.: On the rheology of the upper mantle. Rev. Geophys. Space Phys. **11**, 391–426, 1973

Twiss, R.J.: Structural superplastic creep and linear viscosity in the earth's mantle. Earth Planet. Sci Lett. **33**, 86–100, 1976

Walcott, R.I.: Structure of the earth from glacio-isostatic rebound. Ann. Rev. Earth Planet. Sci. **1**, 15–37, 1973

Weertman, J.: The creep strength of the earth's mantle. Rev. Geophys. Space Phys. **8**, 145–168, 1970

Woollard, G.P.: The interrelationship of crustal and upper mantle parameter values in the Pacific. Rev. Geophys. Space Physics **13**, 87–137, 1975

Yuen, D.A., Tovish, A., Schubert, G.: Shear flow beneath oceanic plates: local nonsimilarity boundary layers for olivine rheology. J. Geophys. Res. **83**, 759–765, 1978